Development 136, 1423-1432 (2009) doi:10.1242/dev.023994

Ptch1 is required locally for mammary gland morphogenesis and systemically for ductal elongation

Ricardo C. Moraes[1], Hong Chang[2], Nikesha Harrington[1], John D. Landua[1], Jonathan T. Prigge[1], Timothy F. Lane[3], Brandon J. Wainwright[4], Paul A. Hamel[2] and Michael T. Lewis[1,*]

Systemic hormones and local growth factor-mediated tissue interactions are essential for mammary gland development. Using phenotypic and transplantation analyses of mice carrying the mesenchymal dysplasia (*mes*) allele of patched 1 (*Ptch1*^{mes}), we found that *Ptch1*^{mes} homozygosity led to either complete failure of gland development, failure of post-pubertal ductal elongation, or delayed growth with ductal dysplasia. All ductal phenotypes could be present in the same animal. Whole gland and epithelial fragment transplantation each yielded unique morphological defects indicating both epithelial and stromal functions for *Ptch1*. However, ductal elongation was rescued in all cases, suggesting an additional systemic function. Epithelial function was confirmed using a conditional null *Ptch1* allele via *MMTV-Cre*-mediated disruption. In *Ptch1*^{mes} homozygotes, failure of ductal elongation correlated with diminished estrogen and progesterone receptor expression, but could not be rescued by exogenous ovarian hormone treatment. By contrast, pituitary isografts were able to rescue the ductal elongation phenotype. Thus, *Ptch1* functions in the mammary epithelium and stroma to regulate ductal morphogenesis, and in the pituitary to regulate ductal elongation and ovarian hormone responsiveness.

KEY WORDS: Hedgehog, SMO, Ductal morphogenesis, Hyperplasia, Pituitary isograft, Tissue interaction, Mouse

INTRODUCTION

Mammary gland development requires both systemic hormones and local growth factor-mediated tissue interactions. Classical hormone ablation/replacement experiments, and more-recent genetic analyses in mice, have shown that post-pubertal gland development requires systemic hormones from ovary [estrogen (E) and progesterone (P)], pituitary [growth hormone (GH) and prolactin (PRL)] and adrenal gland (glucocorticoids) (Topper and Freeman, 1980). Loss of ovarian or pituitary function leads to failure of hormone-dependent ductal elongation after puberty, with E and GH participating primarily in ductal elongation and P and PRL participating primarily in alveolar development. Glucocorticoids enhance (but are not essential for) ductal elongation and are required for alveolar function in lactation.

In addition to systemic hormones, local growth factor signaling, both within and among tissue compartments, is essential for many aspects of normal embryonic and postnatal mammary gland development, as well as for organ maintenance and function in the adult (Sternlicht, 2006; Wiseman and Werb, 2002). For example, insulin-like growth factor 1 (IGF1) functions downstream of GH and PRL to promote ductal elongation. Amphiregulin, a member of the epidermal growth factor (EGF) family, is a major mediator of E-stimulated growth. Other local growth factors contributing to ductal elongation or branching morphogenesis include members of the EGF, fibroblast growth factor (FGF), IGF, Wnt, Notch and TGFβ families, as well as factors such as colony stimulating factor 1 (CSF1), hepatocyte growth factor (HGF), and parathyroid hormone-related protein (PTHrP; PTHLH – Mouse Genome Informatics). Altered tissue interactions mediated by these local growth factors and their receptors contribute significantly to breast pathologies including mastitis and cancer.

In addition to these growth factor signaling systems, one of the primary signaling networks mediating cell-cell interactions during embryonic and postnatal mammary gland development is the hedgehog signaling network (reviewed by Hatsell and Frost, 2007; Lewis and Visbal, 2006). However, it has been unclear in which tissue compartments hedgehog network genes function to regulate gland development, and whether there might be a systemic requirement for hedgehog network gene activity.

In the mouse, mammary gland development begins at about embryonic day 10 (E10) with the induction of the milk line, along which the five pairs of mammary glands will be placed. At E11, mammary placodes (the presumptive nipple) are induced in characteristic positions along the milk line. Induction of the milk line and mammary placodes requires inductive tissue interactions from somites, as well as from a mesodermally derived mammary mesenchyme, to an overlying ectodermally derived epithelium (Chu et al., 2004; Sakakura, 1987; Veltmaat et al., 2003; Veltmaat et al., 2006). Between ~E12 and ~E16, the mammary gland consists of a small bulb of epithelium that begins to invade the fat pad precursor mesenchyme (which gives rise to the mammary fat pad stroma in the postnatal animal) (Hens et al., 2007; Sternlicht, 2006). This early gland development is hormone-independent. At birth, the ductal tree is a rudimentary branched structure, and remains relatively growth quiescent until puberty.

Most mammary gland development occurs after puberty and is under both systemic and local control (Daniel and Silberstein, 1987; Topper and Freeman, 1980). At puberty, systemic reproductive hormones (mainly E and P produced in the ovaries, along with PRL and GH produced in the pituitary) stimulate rapid and invasive ductal elongation driven by growth of the terminal end bud (TEB). Ductal elongation also requires paracrine or juxtacrine cell-cell interactions

[1]Lester and Sue Smith Breast Center and Department of Molecular and Cellular Biology, Baylor College of Medicine, One Baylor Plaza, Houston, TX 77030, USA. [2]Department of Laboratory Medicine and Pathobiology, Faculty of Medicine,1 King's College Circle, University of Toronto, Toronto, Ontario M5S 1A8, Canada. [3]UCLA's Jonsson Comprehensive Cancer Center, 8-684 Factor Building, Box 951781, Los Angeles, CA 90095, USA. [4]Institute for Molecular Bioscience, The University of Queensland, 306 Carmody Road, Brisbane, Queensland 4072, Australia.

*Author for correspondence (e-mail: mtlewis@bcm.edu)

Accepted 19 February 2009

between the epithelial cells themselves (Brisken et al., 1999; Brisken et al., 1998; Mallepell et al., 2006), as well as interactions between the epithelium and surrounding mammary fat pad stroma proper (e.g. fibroblasts, adipocytes) (Sternlicht, 2006; Wiseman and Werb, 2002). Finally, epithelial cells must interact with 'non-mammary' cell types that are produced elsewhere and are recruited into the mammary fat pad. These cell types include vascular cells, macrophages, eosinophils and neuronal cells (Gouon-Evans et al., 2002; Parmely and Manning, 1983; Roubinian and Blair, 1977).

Canonical hedgehog signaling (Cohen, 2003; Evangelista et al., 2006; Hooper and Scott, 2005; Nusse, 2003) typically involves two types of cells, a signaling cell expressing a member of the hedgehog family of secreted ligands [sonic hedgehog (SHH), Indian hedgehog (IHH) or desert hedgehog (DHH)], and a responding cell expressing one or more patched family hedgehog receptors [patched 1 (PTCH1) and patched 2 (PTCH2)]. In the absence of ligand, PTCH1 and PTCH2 can function to inhibit downstream signaling by antagonizing the function of the smoothened (SMO) transmembrane effector protein. Under these conditions, expression of hedgehog target genes is inhibited by repressor forms of one or more members of the Gli family of transcription factors (GLI2 or GLI3). In the presence of ligand, PTCH1 releases inhibition of SMO, which leads to the induction of target genes by transcriptional activator forms of Gli transcription factors (GLI1, GLI2 or GLI3) [detailed models are described in the literature (Cohen, 2003; Evangelista et al., 2006; Hooper and Scott, 2005; Nusse, 2003)].

In addition to its signal transduction activities, PTCH1 can also function to sequester hedgehog ligand, thereby restricting the range over which free ligand can signal (reviewed by Hooper and Scott, 2005). In some cell types, PTCH1 can physically interact with cyclin B1 and inhibit its nuclear entry, thereby preventing cell cell cycle progression (Adolphe et al., 2006; Barnes et al., 2001). Finally, there is evidence to suggest that PTCH1 can function as a 'dependence receptor' to induce apoptosis in cell types that are dependent on ligand-bound PTCH1 for survival (Chao, 2003; Guerrero and Ruiz i Altaba, 2003; Thibert et al., 2003).

We showed previously that two genes, patched 1 (*Ptch1*) and *Gli2*, are required for normal ductal development (Lewis et al., 2001; Lewis et al., 1999; Lewis and Veltmaat, 2004; Lewis and Visbal, 2006). Targeted disruption mutation of either gene leads to ductal dysplasia. Recently, two groups have identified a key role for *Gli3* in the somitic mesenchyme in the FGF10-mediated induction of mammary placodes 3 and 5 (Hatsell and Cowin, 2006; Veltmaat et al., 2006). In the case of *Ptch1*/+, ducts frequently showed ductal hyperplasia with multiple layers of luminal epithelium. Recent work suggests expansion of luminal progenitor cells in this line (Li et al., 2008). Hyperplasias induced by *Ptch1* heterozygosity do not resemble hyperplasias caused by *Smo* activation, which also cause expansion of a progenitor cell pool but lead to alveolar hyperplasia rather than ductal hyperplasia (Lewis et al., 1999; Moraes et al., 2007), indicating that *Ptch1* loss is not functionally equivalent to *Smo* activation. Epithelial fragment transplantation experiments suggested that *Ptch1* functions primarily in the stroma to influence epithelial cell behavior, but epithelial function was not ruled out. However, the mutant phenotype was only partially recapitulated in whole mammary gland transplantation, suggesting that *Ptch1* might have a systemic function as well (Lewis et al., 1999).

To address the tissue compartment-specific requirement for *Ptch1* more fully, we exploited an allelic series of mutations consisting of a targeted disruption allele (*ΔPtch1*) (Goodrich et al., 1997), a conditional disruption allele (*Ptch1*^{c}) (Ellis et al., 2003), as well as the mesenchymal dysplasia (*mes*) allele (Makino et al., 2001) (herein designated *Ptch1*^{mes}), for phenotypic and transplantation analysis of the mouse mammary gland during virgin development. The *Ptch1*^{mes} allele arose as a spontaneous deletion mutation and is haploinsufficient over the null allele, suggesting that it is hypomorphic. However, unlike homozygous *ΔPtch1* mice, which die at E9.5, homozygous *Ptch1*^{mes} mice are viable and show dysplastic growth of mesenchymal tissues, polydactyly, white belly spot, and prior to this study have shown sterility in both sexes. Homozygous *Ptch1*^{mes} pups are initially smaller than their wild-type littermates, but become significantly larger than the wild type by 8-10 weeks of age, consistent with the role of *Ptch1* in body size regulation (Milenkovic et al., 1999).

Using phenotypic and transplantation analyses in conjunction with endocrine manipulation, we find that *Ptch1* is required in both the epithelium and mammary stroma to regulate multiple aspects of gland development. In addition, *Ptch1* functions systemically in the pituitary to promote ductal elongation.

MATERIALS AND METHODS

Animals

Mice were maintained as breeding colonies in our laboratory, and were maintained and used in accordance with the NIH Guide for the Care and Use of Experimental Animals with approval from our Institutional Animal Care and Use Committee.

The *mes* allele of *Ptch1* (*Ptch1*^{mes}) arose spontaneously on the CBA/J background and is the result of a 32 bp deletion in the *Ptch1* locus. This deletion causes a frameshift, such that the resulting PTCH1 protein lacks 271 C-terminal amino acids of the normal protein, which are replaced by 68 unrelated residues. The derivative strain B6C3Fe-a/a-*Ptch1*^{mes}/J (stock number 001430) was obtained for this study. Homozygous *Ptch1*^{mes} mice of both sexes are sterile in this genetic background (Makino et al., 2001).

Two breeding pairs of heterozygous B6C3Fe-a/a-*Ptch1*^{mes}/J mice were used to initiate a breeding colony by serially backcrossing heterozygous males to C57BL/6J females for at least eight generations. Backcross-derived heterozygous mice were then crossed with transgenic mice expressing enhanced cyan fluorescent protein (ECFP) under the chicken β-actin/CMV immediate early enhancer promoter in an inbred C57BL/6J background [strain B6.129(ICR)-Tg(ACTB-ECFP)CK6Nagy/J; stock number 004218] (herein designated *ACTB-ECFP*) (Hadjantonakis et al., 2002) to tag the line genetically to facilitate transplantation experiments and gland imaging. Homozygous *Ptch1*^{mes} females and wild-type controls used experimentally were generated by intercrossing backcross-derived heterozygous mice. Homozygous *Ptch1*^{mes} mice in an inbred C57BL/6J background are poorly fertile, with females frequently failing to deliver viable pups (data not shown).

Ptch1^{mes} mice were genotyped by PCR analysis of tail DNA (DNeasy, Qiagen). Primers used were: forward, 5′-TCCAAGTGTCGTCCGGTTTG-3′; reverse, 5′-GTGGCTTCCACAATCACTTG-3′. 'Step-down' cycling conditions were: 94°C for 60 seconds, 64°C for 30 seconds, and 72°C for 90 seconds (5 cycles), followed by 94°C for 60 seconds, 62°C for 30 seconds, and 72°C for 90 seconds (5 cycles), followed by 94°C for 60 seconds, 60°C for 30 seconds, and 72°C for 90 seconds (25 cycles). A 142 bp product indicated the presence of the wild-type allele, and a 172 bp product indicated the presence of the mutant allele.

Mice carrying a *Ptch1* targeted disruption allele (*Ptch1*^{tm1Mps}, herein designated *ΔPtch1*) were described previously (Goodrich et al., 1997) and were a generous gift from Dr Matthew Scott. The *ΔPtch1* allele was maintained in a C57BL/6J × DBA2 hybrid background by periodic intercrossing with B6D2F1 mice. Genotyping for the disruption allele was modified from that published previously (Goodrich et al., 1997) because of conflicts resulting from the presence of other *Ptch1* alleles. Primers used were: forward, 5′-CAGAGCGGGTAAACTGGCTCGGATTAG-3′; reverse, 5′-TACCGGTGGATGTGGAATGTGTGCG-3′. Conditions were: 94°C for 60 seconds, 57°C for 60 seconds, and 72°C for 90 seconds (35 cycles). A 1100 bp product indicated the presence of the *ΔPtch1* allele.

Mice carrying a *Ptch1 Cre*-recombinase-dependent conditional disruption allele (*Ptch1*^{c}) were described previously (Ellis et al., 2003) and were maintained by serial backcrossing to C57BL/6J. Genotyping for the conditional allele and the recombined allele was performed as described (Ellis et al., 2003).

Mice carrying a *Cre*-recombinase-dependent β-galactosidase (*lacZ*) reporter allele targeted to the *Rosa* locus were described previously (Soriano, 1999) and were obtained from the Jackson Laboratories [strain B6.129S4-*Gt(ROSA)26Sor*^{tm1Sor}/J; stock number 003474] (herein designated R26R) and were maintained by serial backcrossing to C57BL/6J mice. Genotyping for the presence of the *R26R* allele was performed as described (Soriano, 1999).

A transgenic mouse line expressing *Cre* recombinase under the control of the mouse mammary tumor virus (MMTV) promoter (*MMTV-Cre*) was generated previously (Li et al., 2002). Genotyping for the presence of the *MMTV-Cre* transgene was performed as described previously (Li et al., 2002). MMTV-Cre mice were intercrossed with R26R, and backcrossed to C57BL/6J at least once prior to use in this study to allow analysis of mutant phenotypes in a predominately C57BL/6J genetic background.

Immunocompromised B6.129S7-*Rag1*^{tm1Mom}/J (stock number 002216) (herein designated *ΔRag1*) homozygous female mice used as transplantation hosts were not genetically tagged, so as to allow transplanted ECFP-expressing epithelium to be easily distinguished from endogenous epithelium.

Whole gland morphological analysis

For analysis of the *Ptch1*^{mes} allele, homozygous, heterozygous and wild-type littermate or age-matched females were used. Mammary glands #1-5 were harvested from the right side of at least ten female mice at 5 and 10 weeks of age. Additional mice were examined at 20 weeks and at older than 52 weeks of age. Glands were fixed in ice-cold 4% paraformaldehyde in PBS, and examined as whole-mount preparations using Neutral Red staining as described previously (Moraes et al., 2007). Some glands were examined as whole-mount preparations using the ECFP tag for imaging using a Leica MZFL16 fluorescence stereomicroscope equipped with an Optronics Magnafire camera. For display, fluorescence images were exposure-reversed so as to appear similar to Neutral Red-stained preparations. The percentage of fat pad filled was estimated from the whole-mount preparations.

For analysis of the *Ptch1*^{c} allele, we examined glands derived from mice in which *Ptch1* function was conditionally disrupted in the mammary epithelium via *MMTV-Cre*-mediated deletion (Li et al., 2002). To accomplish these analyses, *Ptch1*^{c}*/+; R26R/+* mice were crossed with *ΔPtch1/+; MMTV-Cre/+; R26R* mice to yield the required *Ptch1* genotypes for analysis, either with, or without, *MMTV-Cre*.

For β-galactosidase staining to detect the recombined *R26R* reporter gene, mammary glands were removed and fixed in cold paraformaldehyde for 2 hours, and then stained as described (Ismail et al., 2002). Glands not staining for *lacZ* expression were stained subsequently with Neutral Red (Moraes et al., 2007).

Histology and immunohistochemistry

For histological analysis, the #2 and #3 mammary glands from the left side of the animal were fixed in 4% paraformaldehyde in PBS, embedded in paraffin, sectioned at 3 μm, and either Hematoxylin/Eosin-stained or used for immunolocalization studies. Antibodies against estrogen receptor (ER), progesterone receptor (PR) and BrdU used for immunolocalization studies were as described (Moraes et al., 2007). All immunostaining was performed with antigen retrieval in 0.1 M Tris-HCl (pH 9.0) containing 10% Tween 20, by heating to 120°C for 10 minutes in a pressure cooker. For immunohistochemistry, detection was by standard peroxidase staining using the ABC System (Vector Laboratories).

Whole mammary gland and epithelial fragment transplantation

For transplantation into immunocompromised hosts, *ACTB-ECFP*-tagged epithelial fragments of mammary ducts derived from wild-type and homozygous donor mice were transplanted into epithelium-free 'cleared' #4 fat pads of 3-week-old homozygous *ΔRag1* immunocompromised mice by the method of DeOme (DeOme et al., 1958). Subsequent outgrowths were examined 8 weeks post-transplantation as whole-mounts and histological samples.

For transplantation into immunocompetent hosts, we introgressed the *Ptch1*^{mes} allele into a C57BL/6J inbred background by serial backcross of heterozygous *Ptch1*^{mes}*; ACTB-ECFP* males to C57BL/6J females for at least eight generations. Selected progeny were then tested for histocompatibility by transplantation of epithelial fragments into C57BL/6J hosts. Thereafter, experimental animals were generated by a backcross-intercross strategy, in which backcross-derived heterozygotes were intercrossed to generate homozygous and wild-type mice used for transplantation donors and hosts. For whole gland transplantation, mammary glands from *ACTB-ECFP*-tagged 3-week-old female homozygous *Ptch1*^{mes} or wild-type donors were transplanted between the skin and body wall of 3-week-old female *ΔRag1* host mice between the endogenous #3 and #4 mammary glands (Brisken et al., 1998; Lewis et al., 2001). Transplanted mammary glands were allowed to regenerate ductal trees for 8 weeks. Glands were removed and processed for whole gland and histological analysis.

Ovarian hormone treatments

Virgin mice, at least six per genotype, were treated at 9 weeks of age for a period of 9 days to assay the ability of ovarian hormones to rescue the *Ptch1*^{mes} phenotype and to assay for differential hormone responses. Slow-release implants were constructed of silastic tubing (Cohen and Milligan, 1993) containing either estradiol (E2) alone (20 μg) (Sigma, E-2758), P alone (20 mg) (Sigma, P-130), or E2 and P in combination. Implants were placed under the skin in the suprascapular region. At the end of the treatment period, glands were removed and processed for whole gland and histological analysis.

Pituitary isografts

Virgin mice, at least four per genotype, were transplanted with a single pituitary isograft from a wild-type male donor, or sham-operated as control. The pituitary was placed into the kidney capsule of 4- to 5-week-old host mice (wild-type and *Ptch1*^{mes} homozygous females) as described previously (Said et al., 2001). Three weeks after transplantation, mammary glands were harvested and processed for whole gland and histological analysis.

RESULTS

Ptch1^{mes} is a pleiotropic mutation that affects multiple aspects of mammary ductal development

We showed previously that *ΔPtch1* heterozygosity and *MMTV-SmoM2* transgene overexpression led to two unique mammary hyperplasia phenotypes. Given that the primary function of PTCH1 in the absence of ligand is in downregulation of SMO function (Makino et al., 2001), and that the *Ptch1*^{mes} allele is hypomorphic, we predicted that *Ptch1*^{mes} homozygosity would affect mammary gland ductal development in a manner similar to, but more extensive than, *ΔPtch1* heterozygosity. Alternatively, glands might appear similar to those observed in *MMTV-SmoM2* transgenic mice (which show ductal hyperplasia and increased branching).

To test these predictions, we examined mammary glands of *ACTB-ECFP*-tagged wild-type and homozygous *Ptch1*^{mes} virgin mice at 5, 10 and 20 weeks of age as whole-mount and histological preparations. In whole-mount analysis, at 5 weeks of age glands from wild-type mice showed normal growth, with ~50% of the fat pad filled and multiple TEBs (Fig. 1A). By contrast, 32.4% of glands in *Ptch1*^{mes} homozygotes lacked ductal epithelium entirely (primarily glands #2 and #3) and 59.5% showed severely stunted ductal trees with no TEB present (Fig. 1B). In 8.1% of glands examined, 'escape' ducts formed (Fig. 1C), but in no case did the percentage of fat pad filled approach that of wild-type glands.

At 10 weeks of age, a similar distribution of mammary phenotypes was observed. Whereas glands of wild-type mice were completely filled with a ductal tree and TEBs were completely regressed (Fig. 1D), *Ptch1*^{mes} homozygotes showed 13.3% of glands that lacked mammary epithelium entirely (quantified in Fig. 1J), with 50.5% of glands stunted (Fig. 1E). The escape ducts observed

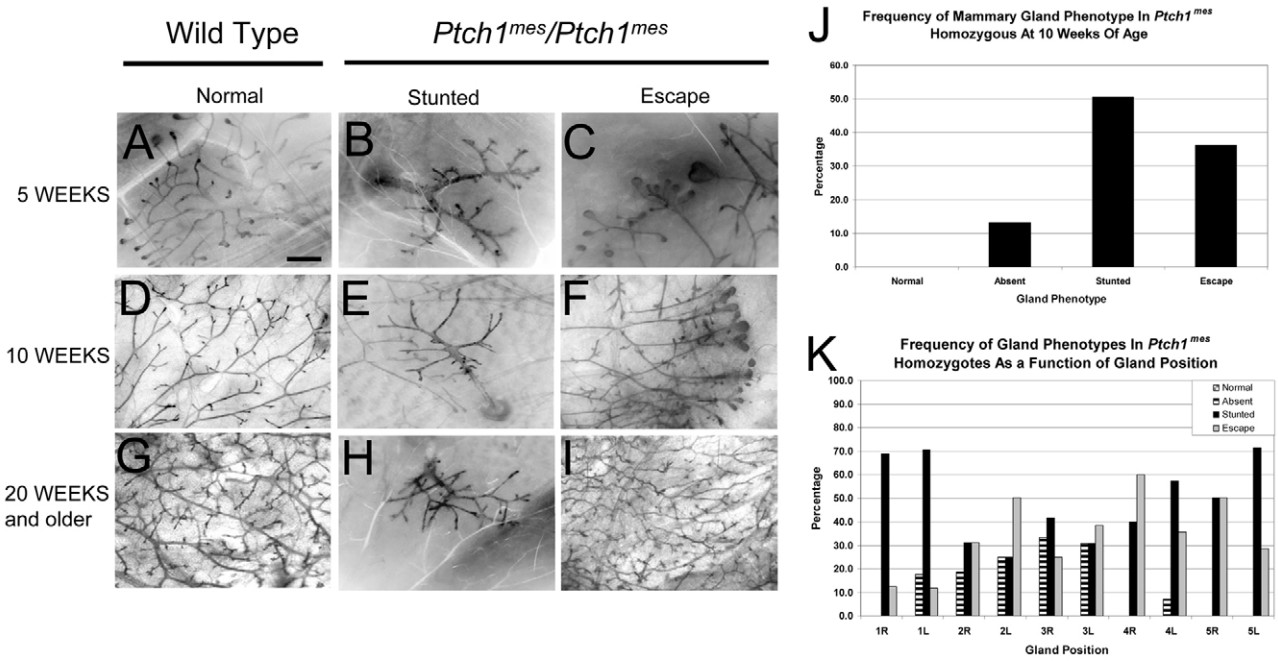

Fig. 1. Whole-mount analysis of mammary glands from wild-type and homozygous *Ptch1*^{mes} mice during postnatal virgin development. The genotype of mice from which glands were derived is shown above each column, along with the phenotype. The developmental timepoint at which glands were harvested is shown to the left. (**A**) Representative ductal tree and terminal end bud (TEB) array in a wild-type mouse at 5 weeks of age showing normal morphology and branching. (**B**) Representative stunted ductal tree in a homozygous *Ptch1*^{mes} mouse. Note the lack of TEBs. (**C**) Representative 'escape' ductal tree and TEB array in a homozygous *Ptch1*^{mes} mouse showing unusual ductal morphology and branching. (**D**) Representative mature ductal tree in a wild-type mouse at 10 weeks of age showing normal morphology and branching. (**E**) The stunted ductal tree inappropriately retained in homozygous *Ptch1*^{mes} mice. (**F**) Representative escape ductal tree and TEB array inappropriately retained in homozygous *Ptch1*^{mes} mice at 10 weeks of age; note the frequently bifurcating and trifurcating TEBs. (**G**) Representative mature ductal tree in a wild-type mouse at 20 weeks of age. (**H**) The stunted ductal tree inappropriately retained in homozygous *Ptch1*^{mes} mice. (**I**) Representative escape ductal tree that completely filled the fat pad in homozygous *Ptch1*^{mes} mice at 20 weeks of age suggesting increased branching. (**J**) Bar chart showing the frequency of gland phenotypes in homozygous *Ptch1*^{mes} mice at 10 weeks of age. (**K**) Bar chart showing the frequency of gland phenotypes as a function of gland position at 10 weeks of age. L, left; R, right. Scale bar: 1 mm.

in 5-week-old mice were also observed in 10-week-old mice (36.2%) (Fig. 1F,J), typically with multiple bifurcating or trifurcating TEBs (Fig. 1F). In no case did we observe a completely filled fat pad. Thus, at the level of whole-mount analysis, glands from *Ptch1*^{mes} homozygotes did not resemble those from *ΔPtch1*/+ heterozygotes (Lewis et al., 1999) or *MMTV-SmoM2* transgenic mice (Moraes et al., 2007).

At 20 weeks of age, glands of wild-type mice were 100% filled, with increased side-branching and alveolar budding relative to 10-week-old mice, and, as at other time points, several glands showed a complete lack of epithelium or remained stunted. However, for some glands, 100% of the fat pad was filled (Fig. 1I).

To characterize the observed gland-to-gland variation in the mammary phenotype, we compared the incidence rates for a given phenotype for gland pairs 1-5 from 16 mice at 10 weeks of age (eight *Ptch1*^{mes} and eight wild type). Fig. 1K summarizes the frequency of mammary gland ductal phenotypes as a function of mammary gland position along the anterior-posterior axis, showing that all glands could be affected, and that ductal elongation varied from gland-to-gland within a given animal.

Abnormalities observed in *ΔPtch1* heterozygotes are partially recapitulated in *Ptch1*^{mes} homozygotes

The most prominent defect observed previously in *ΔPtch1* heterozygotes was partial or complete occlusion of the ducts with multiple layers of luminal epithelial cells. Disorganization of the cap and body cell layers of the TEB was also observed. By histological analysis of *Ptch1*^{mes} homozygous, as compared with wild-type, TEB at 5 weeks of age, stunted ducts showed no histological evidence of a TEB, and no obvious disruption of the epithelium (Fig. 2B versus 2A). By contrast, escape ducts showed some evidence of disruption, particularly in the cap cell layer (Fig. 2C). At 5 weeks of age, escape ducts appeared relatively normal histologically (Fig. 2D versus 2E). At 10 weeks of age, stunted ducts were frequently 3-4 cell layers thick (Fig. 2F), rather than the normal 1-2 cell layers observed in wild-type ducts (Fig. 2E). These ductal dysplasias resembled those seen in *Ptch1*/+ mice (see Fig. 5E,F), but were not as extensive.

Ptch1 functions in both mammary epithelium and stroma

Previous phenotypic and transplantation analyses of *ΔPtch1* heterozygotes suggested that *Ptch1* functions in the stroma to influence epithelial cell function. To determine whether the *Ptch1*^{mes} phenotype observed in intact animals was due to an intrinsic defect in the gland proper, we performed whole gland transplants into immunocompromised *ΔRag1* mice. As expected, glands derived from wild-type mice grew normally (Fig. 3A,C). In contrast to their growth in intact animals, transplanted mammary glands derived from *Ptch1*^{mes} homozygotes grew to similar extents as those from the wild type (Fig. 3B,D), but showed distinct morphological alterations at the duct termini

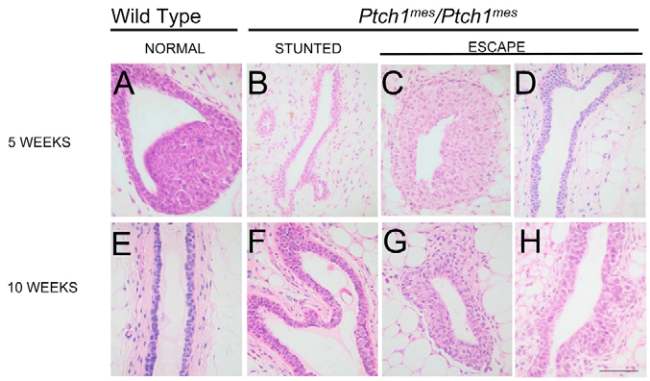

Fig. 2. Histological analysis of glands from wild-type and homozygous *Ptch1*^{mes} mice during postnatal virgin development. The genotype of mice from which glands were derived is shown above each column, along with the phenotype. The developmental timepoint at which glands were harvested is shown to the left. (**A**) A TEB in a gland of a wild-type mouse showing normal histoarchitecture. (**B**) A duct terminus in the stunted ducts of homozygous *Ptch1*^{mes} mice. (**C**) A TEB in a gland from homozygous *Ptch1*^{mes} mice. (**D**) A duct in an escape gland showing a tendency towards increased cell layers and irregular lumen. (**E**) A mature duct in a gland of a wild-type mouse showing normal histoarchitecture. (**F**) A duct in a stunted gland from a homozygous *Ptch1*^{mes} mouse showing multiple layers of luminal epithelial cells. (**G**) A TEB in an escape gland. (**H**) A duct in an escape gland showing generally normal histoarchitecture. Scale bar: 50 μm.

(Fig. 3D). Whole mammary gland transplantation into immunocompetent hosts showed similar results (data not shown). These results suggested that the failure of ductal outgrowth observed in intact *Ptch1* homozygous mutant mice reflected either an early gland-limited defect in gland growth that rendered it in a developmentally arrested state, or a systemic influence of *Ptch1*^{mes} mutation on gland growth.

To determine whether some aspect of the phenotypes observed in *Ptch1*^{mes} mice might be intrinsic to the epithelium, we conducted epithelial fragment transplantation into immunocompromised *ΔRag1* mice. Epithelial fragments from wild-type mice grew as expected, nearly filled the fat pad (Fig. 3E), and showed normal ductal patterning and termini (Fig. 3G). Similarly, and consistent with epithelial growth in whole gland transplantation, epithelial fragments derived from *Ptch1*^{mes} homozygotes grown in the contralateral fat pad grew to a similar extent as those derived from the wild type (Fig. 3F). However, in contrast to glands derived from wild-type mice (Fig. 3G), duct termini from outgrowths derived from *Ptch1*^{mes} homozygotes frequently showed aberrant termini with splayed ends (Fig. 3H). Epithelial fragment transplantation into immunocompetent hosts showed similar results (data not shown). These results demonstrate that *Ptch1* has a function in mammary epithelium to regulate ductal morphogenesis, and indicate that the rounded duct termini observed in whole gland transplants derived from *Ptch1* homozygotes were due to an additional defect in the mammary stroma.

Conditional disruption of *Ptch1* by *MMTV-Cre* confirms an epithelial role for *Ptch1* in mammary ductal morphogenesis

To confirm the epithelial role in mammary gland growth, we examined glands derived from mice in which *Ptch1* function was conditionally disrupted in the mammary epithelium via *MMTV-Cre*-mediated deletion (Li et al., 2002). To accomplish these analyses, *Ptch1*^{c}*/+; R26R/+* mice were crossed with *ΔPtch1/+; MMTV-Cre/+; R26R* mice to yield the required *Ptch1* genotypes for analysis, either with, or without, *MMTV-Cre*. *R26R*-tagged glands that were wild-type for *Ptch1* showed no morphological or histological defects (data not shown). Similarly, mammary glands heterozygous for either *ΔPtch1* (Fig. 4A versus 4B) or *Ptch1*^{c} (Fig. 4C versus 4D) showed no morphological alterations in the presence of *MMTV-Cre*. By contrast, mice carrying both the *Ptch1*^{c} allele and the *ΔPtch1* null allele showed dramatic morphological changes, but only in the presence of *MMTV-Cre* (Fig. 4E versus 4F), including hyperplasia, increased branching and alveolar budding.

In histological analysis, mammary glands heterozygous for either *ΔPtch1* (Fig. 4G versus 4H) or *MMTV-Cre; Ptch1*^{c} (Fig. 4I versus 4J) showed no obvious phenotype; this was unexpected based on our

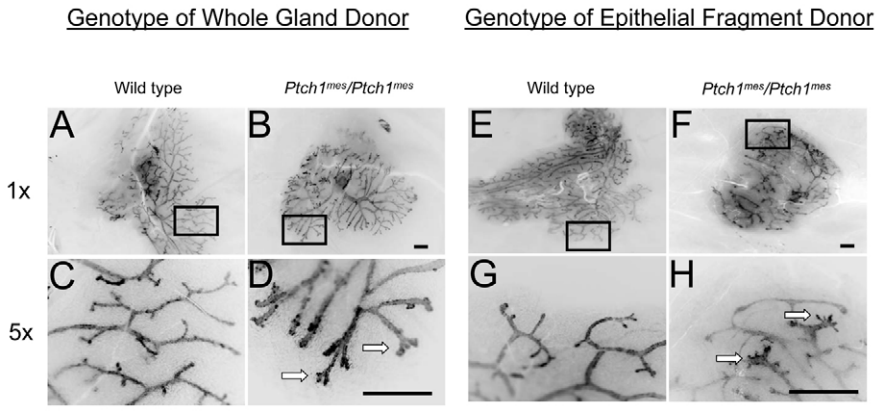

Fig. 3. Whole gland and epithelial fragment transplantation into *Rag1*$^{-/-}$ hosts. The genotype of the epithelial fragment donor is shown above each column, and the magnification values of these inverted fluorescence images to the left. The boxed regions in A,B,E,F are shown at higher magnification in C,D,G,H. (**A**,**C**) Wild-type epithelial fragment showing complete filling of the available fat pad and normal duct morphology (A), with blunt or rounded duct termini (C). (**B**,**D**) Homozygous *Ptch1*^{mes} gland showing complete fat pad filling but modestly altered duct morphology (B), with splayed duct termini (D). (**E**,**G**) Wild-type gland showing complete filling of available fat pad and normal duct morphology (E), with normal blunt or rounded duct termini (G). (**F**,**H**) Homozygous *Ptch1*^{mes} fragment showing complete fat pad filling but modestly altered duct morphology (F), with excessively rounded duct termini (H). Arrows indicate aberrant termini. Scale bars: 1 mm.

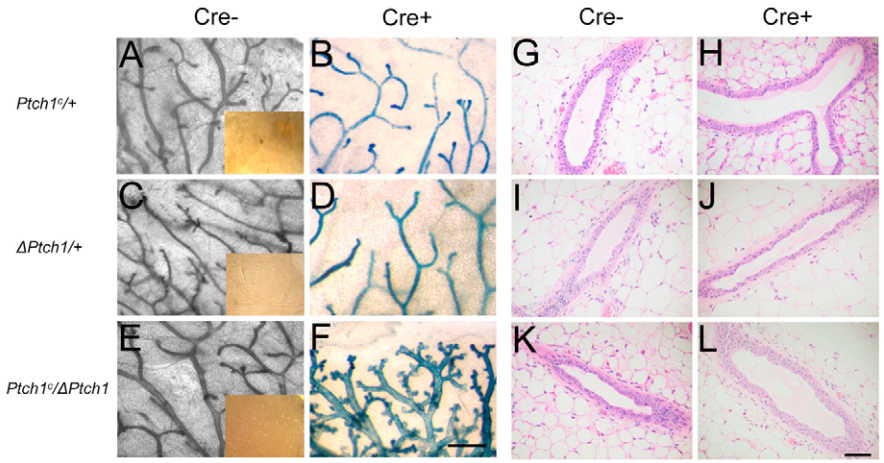

Fig. 4. Whole gland morphological and histological analysis of the *Ptch1* conditional null allele at 10 weeks of age. (**A-F**) Carmine (A,C,E) and *lacZ* (B,D,F) staining of whole glands of mice that were either negative (*Cre*–) or positive (*Cre*+) for *Cre* recombinase expression; magnification, 5×. Mice were interbred with R26R mice and with a separate trangenic strain expressing *Cre* recombinase under the transcriptional control of the MMTV promoter region. Insets represent *lacZ*-stained glands from mice that were *Cre* negative; magnification, 1×. (**G-L**) Histological analysis of mice that were either negative or positive for *Cre* recombinase expression. Scale bars: 0.5 mm in A-F; 50 μm in G-L.

previously published work. By contrast, mice carrying both the $Ptch1^{c}$ allele and the *ΔPtch1* allele showed histological changes, with some ducts showing more than two layers of luminal epithelial cells, but only in the presence of *MMTV-Cre* (Fig. 4K versus 4L). Thus, the phenotype of $Ptch1^{c}$/*ΔPtch1* was similar to, but less extensive than, that of *ΔPtch1* heterozygosity in a B6D2F1 background.

Morphological changes caused by *ΔPtch1* heterozygosity are background dependent

During the course of the analysis of the $Ptch1^{c}$ allele, we noted that *ΔPtch1* heterozygosity in a predominantly C57BL/6J genetic background did not lead to the same phenotypes that we observed previously in a C57BL/6J × DBA2 hybrid genetic background. To investigate a possible background influence on defects induced by *ΔPtch1*, we backcrossed C57BL/6J × DBA2 hybrid male mice carrying the *ΔPtch1* target disruption allele with wild-type females of different backgrounds (B6D2F1, C57BL/6J, DBA2 and FVB) for at least four generations. The mammary gland developed normally in all wild-type mice, and in a manner characteristic for each given strain (Fig. 5A-D). *ΔPtch1* heterozygosity led to the previously described histological alterations in both the B6D2F1 and DBA2 backgrounds (Fig. 5E,F), in which ducts were present with multiple layers of luminal cells that almost obstructed the ductal lumen (Lewis et al., 1999). No histological defects were observed in the FVB or C57BL/6J backgrounds (Fig. 5G,H).

As expected, BrdU incorporation was low in wild-type glands from all backgrounds, except DBA2, which showed a slightly elevated average BrdU labeling index in wild-type mice (Fig. 5I-L and see Fig. 7). Consistent with the observed histological defects in B6D2F1 and DBA2 *ΔPtch1* heterozygotes, we observed a statistically significant increase in proliferation in the B6D2F1 and DBA2 backgrounds, but not in the C57BL/6J and FVB backgrounds (Fig. 5M-P). Fig. 5Q summarizes changes the in proliferation as a function of genetic background and *ΔPtch1* heterozygosity.

Recently, a polymorphism in *Ptch1* was linked with resistance to *Hras*-induced squamous carcinoma of the skin in C57BL/6J relative to FVB mice (Wakabayashi et al., 2007). To investigate the possibility that this polymorphism was responsible for the strain differences we observed, we sequenced the polymorphic region in each inbred strain. The A→C polymorphism was present in C57BL/6J, but was not observed in either FVB or DBA2. Since a statistically significant increase in proliferation was only observed in DBA2, but not FVB, this polymorphism cannot account for the increase in proliferation observed in the DBA2 strain (Fig. 6), thus implicating a genetic modifier of *Ptch1* in the DBA2 strain.

Duct growth is not rescued by exogenous estrogen or progesterone

Gland-to-gland variability in an individual animal was not entirely consistent with a systemic hormonal defect, yet stunted duct growth in $Ptch1^{mes}$ homozygotes was reminiscent of mice carrying loss-of-function mutations in estrogen receptor α (ERα) (Korach, 1994; Mallepell et al., 2006). To test the ability of ovarian hormones to rescue the stunted growth phenotype, we treated wild-type and homozygous mutant mice with E2 alone, P alone, or both (E2+P), and compared them with untreated animals. Untreated wild-type animals showed normal gland morphology, with little alveolar development (Fig. 7A); there was increased alveolar budding with E2 alone (Fig. 7B), P alone (Fig. 7C), and E2+P treatments (Fig. 7D). By contrast, the stunted glands of $Ptch1^{mes}$ homozygotes showed little or no evidence of response to any treatment (Fig. 7H, inset). However, escape ducts (Fig. 7F versus Fig. 6H) did show evidence of hormone responsiveness, with E2 alone (Fig. 7F), P alone (Fig. 7G) and E2+P (Fig. 7H) causing increased side-branching and alveolar budding, such that they approached levels seen in wild-type mice.

To investigate further the reason for the differential hormone responses of stunted versus escape ducts in $Ptch1^{mes}$ homozygotes, we conducted an immunohistochemical analysis of ER and progesterone receptor (PR) expression, as well as of BrdU incorporation as an index of proliferation. Wild-type glands showed the anticipated 36.1% of luminal epithelial cells expressing ER (Fig. 7I). By contrast, in stunted ducts of $Ptch1^{mes}$ homozygotes, ER expression was greatly reduced (Fig. 7J), with fewer cells expressing detectable receptor. Escape ducts also showed reduced ER expression (Fig. 7K) and an intermediate percentage of cells expressing detectable ER. PR showed a similar pattern of expression to ER (Fig. 7L,M). This reduced expression of both receptors was consistent with the reduced hormone responsiveness observed.

With respect to proliferation, untreated wild-type glands showed 0.5% BrdU labeling (Fig. 7O). Similarly, untreated stunted ducts of $Ptch1^{mes}$ homozygotes showed only 0.5% BrdU labeling (Fig. 7P), and untreated escape ducts of $Ptch1^{mes}$ homozygotes showed 7.2% BrdU labeling (Fig. 7Q). We detected a significant increase in BrdU incorporation caused by $Ptch1^{mes}$ only in glands expressing the near-normal range of estrogen receptors.

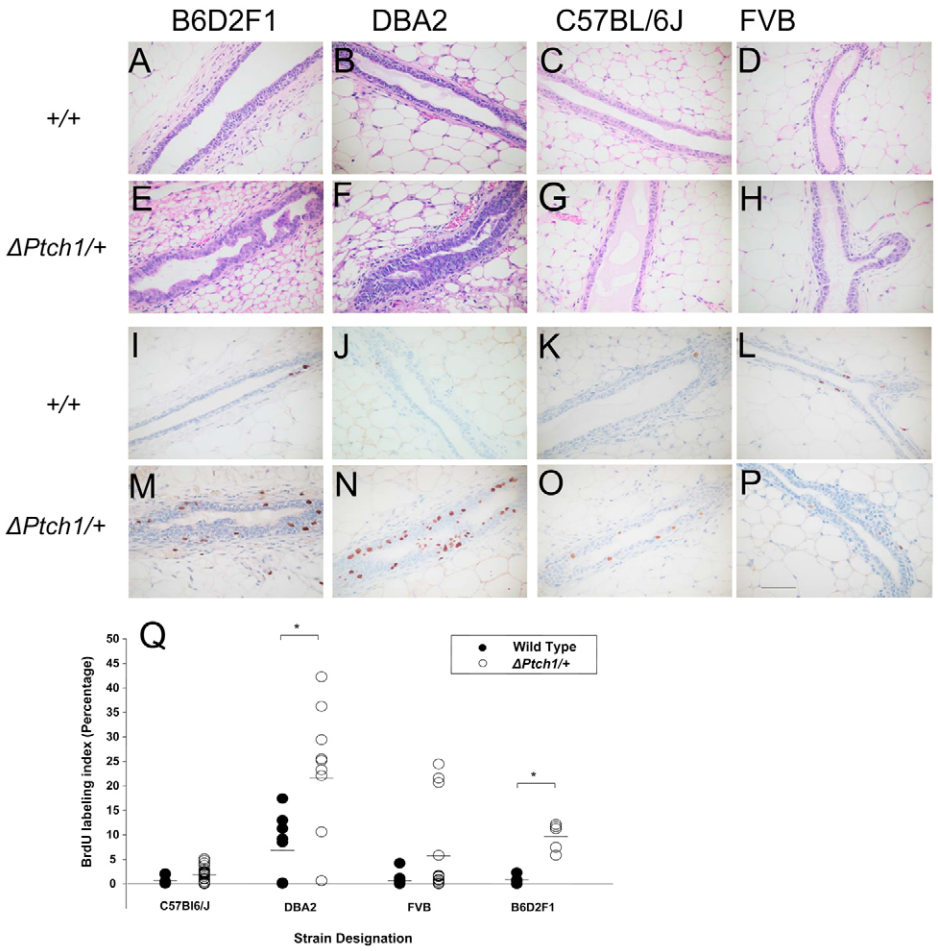

Fig. 5. Effect of *ΔPtch1* heterozygosity in different genetic backgrounds. The mouse background is shown above each column, the genotype to the left. (**A-H**) Hematoxylin/Eosin-stained sections of mammary gland. (**I-P**) BrdU staining for evaluation of proliferation. (**Q**) BrdU labeling index for wild type and *ΔPtch1*/+ in different backgrounds. **P*=0.017 and **P*=0.024 for DBA2 and B6D2F1, respectively (Wilcoxon rank sum test). Scale bar: 50 μm.

Ductal elongation defects caused by *Ptch1*^{mes} homozygosity are rescued by pituitary isograft

To determine whether the ductal elongation failure in *Ptch1*^{mes} homozygotes could be rescued by pituitary hormones, we transplanted a single pituitary into *Ptch1*^{mes} and wild-type host animals at 4-5 weeks of age. Three weeks after transplantation, sham-operated wild-type animals showed ductal elongation characteristic of 7- to 8-week-old virgin mice, with extensive ductal elongation and visible TEBs (Fig. 8A). Wild-type animals hormonally stimulated by pituitary isografts exhibited a significant increase in ductal elongation, branching and alveolar development (Fig. 8B), with no TEBs remaining, and ducts reaching the periphery of the fat pad. Sham-operated *Ptch1*^{mes} homozygotes showed the expected stunted or modest escape duct growth (Fig. 8C). However, *Ptch1*^{mes} homozygotes receiving a pituitary transplant showed significantly enhanced ductal elongation (Fig. 8D), with prominent TEBs and an average of ~55% of the fat pad filled (in contrast to an average of ~26% in sham-operated homozygotes) (Fig. 8). These results indicate that *Ptch1* function is required in the pituitary to drive ductal elongation and control hormone responsiveness.

DISCUSSION

It is not currently known in which tissue compartment(s) and cell type(s) *Ptch1* function is required for normal mammary gland development, nor is it known which of the five or more functions of *Ptch1* may be acting in a given location.

Our previous analysis of a *Ptch1* loss-of-function allele (*ΔPtch1*) in a mixed genetic background (C57BL/6J × DBA2) demonstrated that heterozygous loss of *Ptch1* in mouse led to increased proliferation and ductal dysplasias similar to ductal hyperplasias of the human breast. Transplantation of epithelial fragments into cleared fat pads of immunocompromised (*Rag1*$^{-/-}$) or B6D2F1 host mice did not recapitulate the phenotype observed in intact animals. By contrast, whole mammary gland transplantation into immunocompromised or B6D2F1 host mice achieved a partial recapitulation of the mutant phenotype. These data led to the interpretation that *Ptch1* functions primarily in the stroma to direct epithelial cell behavior. However, epithelial and systemic functions of *Ptch1* were not ruled out.

Fig. 6. Genetic polymorphism in the *Ptch1* gene. (**A**) Partial gene sequence of *Ptch1* from human, FVB, C57BL/6J and DBA2 mice. (**B**) Partial amino acid sequence of patched protein from human, FVB, C57BL/6J and DBA2 mice. The boxed residues indicate the A→C polymorphism (A) and resulting amino acid substitution (B) in the PTCH1 protein.

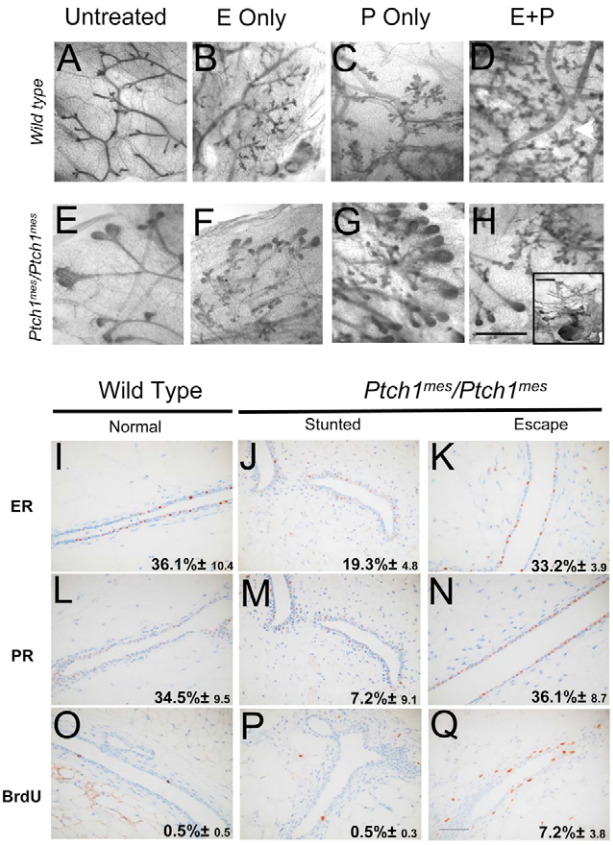

Fig. 7. Ovarian hormone treatment assays to evaluate hormone responsiveness and immunohistochemical analysis for expression of ER and PR and for BrdU incorporation as a function of genotype and phenotype. (**A-H**) Treatment is shown above each column, the genotype of the treated mice to the left. (A) Wild type, untreated. (B) Wild type, E2-treated, showing increased branching and alveolar development. (C) Wild type, P-treated, showing increased branching and alveolar development. (D) Wild type, E2+P-treated, showing increased branching and alveolar development. (E) Homozygous *Ptch1*^{mes} escape gland showing retained TEBs. (F) Homozygous *Ptch1*^{mes} escape gland, E2-treated, showing a comparable response to the wild type (B). (G) Homozygous *Ptch1*^{mes} escape gland, P-treated, showing a comparable response to the wild type (C). (H) Homozygous *Ptch1*^{mes} escape gland, E2+P-treated, showing a comparable response to the wild type. The inset shows a stunted gland in a homozygous *Ptch1*^{mes} showing no responsiveness to E2+P. (**I-Q**) Immunohistochemical analysis for expression of estrogen receptor (ER) and progesterone receptor (PR), and for BrdU incorporation as a function of genotype and phenotype. Scale bars: 2 mm in A-H; 50 μm in I-Q.

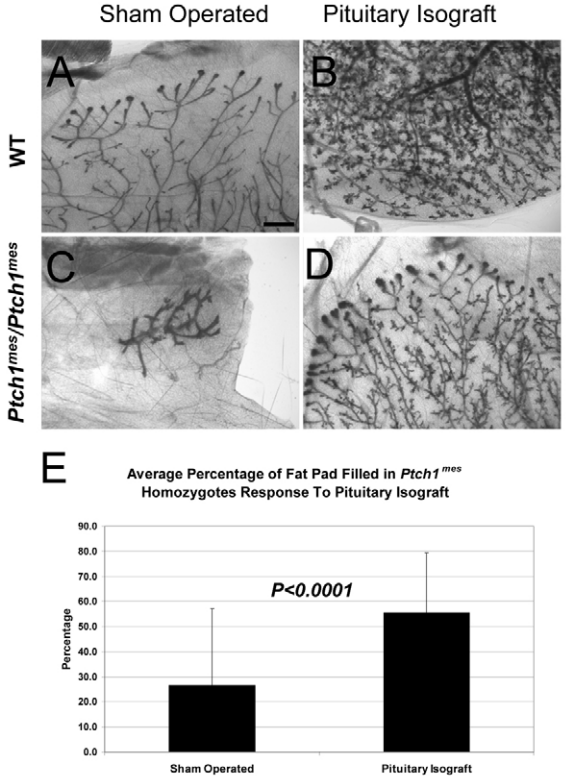

Fig. 8. Whole-mount analysis of mammary glands from mice wild-type for *Ptch1* and from *Ptch1*^{mes}/*Ptch1*^{mes} mice after pituitary isograft transplant. (**A**) Representative ductal tree in a mouse wild-type for *Ptch1* (WT) at 8 weeks of age showing normal morphology and branching. (**B**) Representative WT ductal tree after pituitary isograft. Note the alveolar development and ducts reaching the fat pad periphery. (**C**) Stunted ductal tree in a sham-operated *Ptch1*^{mes}/*Ptch1*^{mes} mouse. (**D**) Representative *Ptch1*^{mes}/*Ptch1*^{mes} mammary gland showing ductal and alveolar development after pituitary isograft. (**E**) Bar chart showing the percentage of fat pad filled in *Ptch1*^{mes}/*Ptch1*^{mes} animals. Scale bar: 1 mm.

In this study, we exploited two additional novel *Ptch1* alleles to elucidate the roles of *Ptch1* in virgin mammary gland development more fully. Using the hypomorphic *Ptch1*^{mes} allele, we demonstrate that homozygosity leads to three main phenotypes in intact animals: (1) the complete absence of mammary epithelium; (2) a failure of ductal elongation leading to persistence of stunted, rudimentary glands similar to those observed in wild-type mice prior to puberty; or (3) dysplastic growth of escape ducts, which fail to fill the available fat pad by 10 weeks of age despite increased proliferation. All three phenotypes may be present in the same animal. Whole gland and epithelial transplantation showed that *Ptch1* has functions in both the mammary epithelium and mammary stroma. However, the stunted growth phenotype was fully rescued by transplantation in all cases, indicating a systemic function.

Using the *Ptch1*^{c} allele in combination with the *ΔPtch1* allele analyzed previously, we now confirm a key role for epithelial *Ptch1* in regulating ductal morphogenesis. However, the dysplastic duct histoarchitecture observed previously was not fully recapitulated when *Ptch1* was disrupted solely in the epithelium in *Ptch1*^{c}/*ΔPtch1* mice, nor was it observed in a mixed genetic background. Although loss of *Ptch1* function solely in mammary epithelium led to ductal dysplasia, this phenotype was distinctly different from the alveolar hyperplasias induced by ectopic expression of activated SMO in *MMTV-SmoM2* transgenic mice. Thus, PTCH1 loss-of-function is not functionally equivalent to SMO activation in mammary epithelium, suggesting that PTCH1 might have SMO-independent functions in the gland.

In virgin female *Ptch1*^{mes} homozygous mice, we show that ~30% of animals have one or more mammary glands that entirely lack mammary epithelium. Although we have not yet investigated whether this phenotype is due to a failure of development in the embryo, lack of mammary structures is similar to the embryonic phenotype of *ΔGli3* homozygotes, in which mammary glands #3

and #5 fail to develop (Hatsell and Cowin, 2006; Veltmaat et al., 2006). GLI3 repressor function is required in the somites underlying the #3 mammary glands to allow FGF10 signaling to the overlying ectoderm to induce a mammary placode. It will be of considerable interest to determine whether the *Ptch1*^{mes} phenotype is indeed due to a similar failure to induce FGF10 signaling, with a broader position specificity than *Gli3* loss-of-function.

The ability of transplantation to rescue the stunted duct growth phenotype suggested a systemic role for *Ptch1* in regulating gland development. If a defect is intrinsic to the epithelial compartment [e.g. disruption of the estrogen receptor α gene (*Erα*; *Esr1* – Mouse Genome Informatics) (Mallepell et al., 2006)], one expects the mutant phenotype to be recapitulated in epithelial fragment transplantation. If a defect is intrinsic to the mammary gland stromal compartment proper [e.g. disruption of the parathyroid hormone-related peptide receptor (PTHR1; PTH1R – Mouse Genome Informatics) (Dunbar et al., 1998)], one would expect the phenotype to be recapitulated in whole mammary gland transplants. Although we observed minor morphological alterations under these two conditions, mammary duct outgrowth was rescued in all cases, thereby demonstrating a systemic role for PTCH1. Using classical hormone treatment, we now show that *Ptch1* is required in the pituitary for ductal elongation and hormone responsiveness.

The pituitary gland produces two hormones required for gland development, GH and PRL. GH acts on mammary stroma to produce IGF1, which in turn acts on mammary epithelium to promote ductal outgrowth. PRL also facilitates ductal morphogenesis via IGF1, and regulates ER and PR expression (Frasor and Gibori, 2003; Muldoon, 1987), but is primarily responsible for driving alveolar development and function during pregnancy and lactation (Ormandy et al., 1997). Preliminary experiments indicate that neither GH nor PRL treatment alone is sufficient to rescue the growth of mammary glands in *Ptch1*^{mes} homozygotes, suggesting that a combinatorial function of pituitary-derived factors is required to promote ductal elongation and hormone responsiveness. We are currently exploring whether treatment with IGF1, amphiregulin and/or PTHrP is capable of altering the *Ptch1*^{mes} homozygous phenotype, either alone or in combination. We are also testing whether forced expression of ERα in *MMTV-Erα* or of IGF1 in *MMTV-Igf1* transgenic mice will rescue the stunted growth phenotype.

Finally, we demonstrate that the *ΔPtch1/+* hyperplastic phenotype described previously (Lewis et al., 1999; Moraes et al., 2007) is dependent on genetic background, with B6D2F1 and DBA2 mice expressing the mutant phenotype, whereas C57BL/6J and FVB mice do not show hyperplasia. The hyperplastic phenotype was also observed recently in a C57BL/6J/129 mixed genetic background (Li et al., 2008). These results provide an explanation for why two other groups did not observe a dysplastic phenotype in their alternative genetic backgrounds (Fiaschi et al., 2007; Hatsell and Frost, 2007). Recently, a polymorphic variant in the *Ptch1* gene has been identified in C57BL/6J versus FVB mice, the presence of which correlates with either resistance (C57BL/6J) or susceptibility (FVB) of mice to *Hras*-induced squamous cell carcinoma of the skin (Wakabayashi et al., 2007). This polymorphism cannot account fully for our observations, given that the ductal dysplasia phenotype was not observed in the FVB background, but was observed in DBA2 despite the presence of the same allelic variant. However, the disparity observed in the backgrounds might be explained by the presence of a genetic modifier in DBA and B6D2F1, which may be acting synergistically with the deletion of the *Ptch1* gene to induce higher levels of cellular proliferation.

This work was supported by the National Institutes of Health grants P01-CA30195 and R01- CA127857 (M.T.L.), and partially supported through a joint program of the Canadian Breast Cancer Research Alliance, the National Cancer Institute of Canada and the Canadian Institutes of Health Research (MOP-49614) (P.A.H.). Deposited in PMC for immediate release.

References

Adolphe, C., Hetherington, R., Ellis, T. and Wainwright, B. (2006). Patched1 functions as a gatekeeper by promoting cell cycle progression. *Cancer Res.* **66**, 2081-2088.
Barnes, E. A., Kong, M., Ollendorff, V. and Donoghue, D. J. (2001). Patched1 interacts with cyclin B1 to regulate cell cycle progression. *EMBO J.* **20**, 2214-2223.
Brisken, C., Park, S., Vass, T., Lydon, J. P., O'Malley, B. W. and Weinberg, R. A. (1998). A paracrine role for the epithelial progesterone receptor in mammary gland development. *Proc. Natl. Acad. Sci. USA* **95**, 5076-5081.
Brisken, C., Kaur, S., Chavarria, T. E., Binart, N., Sutherland, R. L., Weinberg, R. A., Kelly, P. A. and Ormandy, C. J. (1999). Prolactin controls mammary gland development via direct and indirect mechanisms. *Dev. Biol.* **210**, 96-106.
Chao, M. V. (2003). Dependence receptors: what is the mechanism? *Sci. STKE* **2003**, PE38.
Chu, E. Y., Hens, J., Andl, T., Kairo, A., Yamaguchi, T. P., Brisken, C., Glick, A., Wysolmerski, J. J. and Millar, S. E. (2004). Canonical WNT signaling promotes mammary placode development and is essential for initiation of mammary gland morphogenesis. *Development* **131**, 4819-4829.
Cohen, M. M., Jr (2003). The hedgehog signaling network. *Am. J. Med. Genet.* **123A**, 5-28.
Cohen, P. E. and Milligan, S. R. (1993). Silastic implants for delivery of oestradiol to mice. *J. Reprod. Fertil.* **99**, 219-223.
Daniel, C. W. and Silberstein, G. B. (1987). Developmental biology of the mammary gland. In *The Mammary Gland* (ed. M. C. Neville and C. W. Daniel). New York: Plenum.
DeOme, K. B., Faulkin, L. J. J. and Bern, H. (1958). Development of mammary tumors from hyperplastic alveolar nodules transplanted into gland-free mammary fat pads of female C3H mice. *Cancer Res.* **19**, 515-520.
Dunbar, M. E., Young, P., Zhang, J. P., McCaughern-Carucci, J., Lanske, B., Orloff, J. J., Karaplis, A., Cunha, G. and Wysolmerski, J. J. (1998). Stromal cells are critical targets in the regulation of mammary ductal morphogenesis by parathyroid hormone-related protein. *Dev. Biol.* **203**, 75-89.
Ellis, T., Smyth, I., Riley, E., Graham, S., Elliot, K., Narang, M., Kay, G. F., Wicking, C. and Wainwright, B. (2003). Patched 1 conditional null allele in mice. *Genesis* **36**, 158-161.
Evangelista, M., Tian, H. and de Sauvage, F. J. (2006). The hedgehog signaling pathway in cancer. *Clin. Cancer Res.* **12**, 5924-5928.
Fiaschi, M., Rozell, B., Bergstrom, A., Toftgard, R. and Kleman, M. I. (2007). Targeted expression of GLI1 in the mammary gland disrupts pregnancy-induced maturation and causes lactation failure. *J. Biol. Chem.* **282**, 36090-36101.
Frasor, J. and Gibori, G. (2003). Prolactin regulation of estrogen receptor expression. *Trends Endocrinol. Metab.* **14**, 118-123.
Goodrich, L. V., Milenkovic, L., Higgins, K. M. and Scott, M. P. (1997). Altered neural cell fates and medulloblastoma in mouse patched mutants. *Science* **277**, 1109-1113.
Gouon-Evans, V., Lin, E. Y. and Pollard, J. W. (2002). Requirement of macrophages and eosinophils and their cytokines/chemokines for mammary gland development. *Breast Cancer Res.* **4**, 155-164.
Guerrero, I. and Ruiz i Altaba, A. (2003). Development: longing for ligand: hedgehog, patched, and cell death. *Science* **301**, 774-776.
Hadjantonakis, A. K., Macmaster, S. and Nagy, A. (2002). Embryonic stem cells and mice expressing different GFP variants for multiple non-invasive reporter usage within a single animal. *BMC Biotechnol.* **2**, 11.
Hatsell, S. J. and Cowin, P. (2006). Gli3-mediated repression of Hedgehog targets is required for normal mammary development. *Development* **133**, 3661-3670.
Hatsell, S. and Frost, A. R. (2007). Hedgehog signaling in mammary gland development and breast cancer. *J. Mammary Gland Biol. Neoplasia* **12**, 163-173.
Hens, J. R., Dann, P., Zhang, J. P., Harris, S., Robinson, G. W. and Wysolmerski, J. (2007). BMP4 and PTHrP interact to stimulate ductal outgrowth during embryonic mammary development and to inhibit hair follicle induction. *Development* **134**, 1221-1230.
Hooper, J. E. and Scott, M. P. (2005). Communicating with Hedgehogs. *Nat. Rev. Mol. Cell Biol.* **6**, 306-317.
Ismail, P. M., Li, J., DeMayo, F. J., O'Malley, B. W. and Lydon, J. P. (2002). A novel LacZ reporter mouse reveals complex regulation of the progesterone receptor promoter during mammary gland development. *Mol. Endocrinol.* **16**, 2475-2489.
Korach, K. S. (1994). Insights from the study of animals lacking functional estrogen receptor. *Science* **266**, 1524-1527.
Lewis, M. T. and Veltmaat, J. M. (2004). Next stop, the twilight zone: hedgehog network regulation of mammary gland development. *J. Mammary Gland Biol. Neoplasia* **9**, 165-181.

Lewis, M. T. and Visbal, A. P. (2006). The hedgehog signaling network, mammary stem cells, and breast cancer: connections and controversies. *Ernst Schering Found. Symp. Proc.* **5**, 181-217.
Lewis, M. T., Ross, S., Strickland, P. A., Sugnet, C. W., Jimenez, E., Scott, M. P. and Daniel, C. W. (1999). Defects in mouse mammary gland development caused by conditional haploinsufficiency of Patched-1. *Development* **126**, 5181-5193.
Lewis, M. T., Ross, S., Strickland, P. A., Sugnet, C. W., Jimenez, E., Hui, C. and Daniel, C. W. (2001). The Gli2 transcription factor is required for normal mouse mammary gland development. *Dev. Biol.* **238**, 133-144.
Li, G., Robinson, G. W., Lesche, R., Martinez-Diaz, H., Jiang, Z., Rozengurt, N., Wagner, K. U., Wu, D. C., Lane, T. F., Liu, X. et al. (2002). Conditional loss of PTEN leads to precocious development and neoplasia in the mammary gland. *Development* **129**, 4159-4170.
Li, N., Singh, S., Cherukuri, P., Li, H., Yuan, Z., Ellisen, L. W., Wang, B., Robbins, D. and DiRenzo, J. (2008). Reciprocal intraepithelial interactions between TP63 and hedgehog signaling regulate quiescence and activation of progenitor elaboration by mammary stem cells. *Stem Cells* **26**, 1253-1264.
Makino, S., Masuya, H., Ishijima, J., Yada, Y. and Shiroishi, T. (2001). A spontaneous mouse mutation, mesenchymal dysplasia (mes), is caused by a deletion of the most C-terminal cytoplasmic domain of patched (ptc). *Dev. Biol.* **239**, 95-106.
Mallepell, S., Krust, A., Chambon, P. and Brisken, C. (2006). Paracrine signaling through the epithelial estrogen receptor {alpha} is required for proliferation and morphogenesis in the mammary gland. *Proc. Natl. Acad. Sci. USA* **103**, 2196-2201.
Milenkovic, L., Goodrich, L. V., Higgins, K. M. and Scott, M. P. (1999). Mouse patched1 controls body size determination and limb patterning. *Development* **126**, 4431-4440.
Moraes, R. C., Zhang, X., Harrington, N., Fung, J. Y., Wu, M. F., Hilsenbeck, S. G., Allred, D. C. and Lewis, M. T. (2007). Constitutive activation of smoothened (Smo) in mammary glands of transgenic mice leads to increased proliferation, altered differentiation and ductal dysplasia. *Development* **134**, 1231-1242.
Muldoon, T. G. (1987). Prolactin mediation of estrogen-induced changes in mammary tissue estrogen and progesterone receptors. *Endocrinology* **121**, 141-149.
Nusse, R. (2003). Wnts and Hedgehogs: lipid-modified proteins and similarities in signaling mechanisms at the cell surface. *Development* **130**, 5297-5305.
Ormandy, C. J., Binart, N. and Kelly, P. A. (1997). Mammary gland development in prolactin receptor knockout mice. *J. Mammary Gland Biol. Neoplasia* **2**, 355-364.
Parmely, M. J. and Manning, L. S. (1983). Cellular determinants of mammary cell-mediated immunity in the rat: kinetics of lymphocyte subset accumulation in the rat mammary gland during pregnancy and lactation. *Ann. New York Acad. Sci.* **409**, 517-533.
Roubinian, J. R. and Blair, P. B. (1977). Inhibition of mammary tumors by incomplete T-cell depletion. *J. Natl. Cancer Inst.* **58**, 727-734.
Said, T. K., Moraes, R. C., Singh, U., Kittrell, F. S. and Medina, D. (2001). Cyclin-dependent kinase (cdk) inhibitors/cdk4/cdk2 complexes in early stages of mouse mammary preneoplasia. *Cell Growth Differ.* **12**, 285-295.
Sakakura, T. (1987). Mammary embryogenesis. In *The Mammary Gland* (ed. M. C. Neville and C. W. Daniel). New York: Plenum.
Soriano, P. (1999). Generalized lacZ expression with the ROSA26 Cre reporter strain. *Nat. Genet.* **21**, 70-71.
Sternlicht, M. D. (2006). Key stages in mammary gland development: the cues that regulate ductal branching morphogenesis. *Breast Cancer Res.* **8**, 201.
Thibert, C., Teillet, M. A., Lapointe, F., Mazelin, L., Le Douarin, N. M. and Mehlen, P. (2003). Inhibition of neuroepithelial patched-induced apoptosis by sonic hedgehog. *Science* **301**, 843-846.
Topper, Y. J. and Freeman, C. S. (1980). Multiple hormone interactions in the developmental biology of the mammary gland. *Physiol. Rev.* **60**, 1049-1106.
Veltmaat, J. M., Mailleux, A. A., Thiery, J. P. and Bellusci, S. (2003). Mouse embryonic mammogenesis as a model for the molecular regulation of pattern formation. *Differentiation* **71**, 1-17.
Veltmaat, J. M., Relaix, F., Le, L. T., Kratochwil, K., Sala, F. G., van Veelen, W., Rice, R., Spencer-Dene, B., Mailleux, A. A., Rice, D. P. et al. (2006). Gli3-mediated somitic Fgf10 expression gradients are required for the induction and patterning of mammary epithelium along the embryonic axes. *Development* **133**, 2325-2335.
Wakabayashi, Y., Mao, J. H., Brown, K., Girardi, M. and Balmain, A. (2007). Promotion of Hras-induced squamous carcinomas by a polymorphic variant of the Patched gene in FVB mice. *Nature* **445**, 761-765.
Wiseman, B. S. and Werb, Z. (2002). Stromal effects on mammary gland development and breast cancer. *Science* **296**, 1046-1049.